Dye Transfer between Cells of the Embryonic Chick Lens Becomes Less Sensitive to CO_2 Treatment with Development

STEPHEN M. SCHUETZE and DANIEL A. GOODENOUGH
Department of Anatomy Harvard Medical School, Boston, Massachusetts 02115. Dr. Schuetze's present address is Department of Biological Sciences, Columbia University, New York 10027.

ABSTRACT During the 3-h developmental stage 14 in the chick, intercellular transfer of iontophoresed fluorescent dyes becomes less sensitive to the lowering of intracellular pH by either CO_2 or acetate ions. Up to developmental stage 14, dye transfer between lens cells is reversibly blocked by exposure to 50% CO_2. Beyond stage 14, dye transfer between these cells is no longer reversibly blocked by elevated pCO_2. Electrotonic coupling is present throughout lens development and is not reversibly blocked by high pCO_2 at any stage. The gap junctions joining the lens cells show morphological changes at developmental stage 14. Up to stage 14, all gap junctions observed between chick lens cells have connexon assemblies that appear condensed or crystalline following routine freeze-fracture microscopy. Beyond stage 14, chick lens cells express gap junctions with both the condensed assemblies and the dispersed assemblies characteristic of adult lens gap-junction structure.

Gap junctions joining adult lens fibers differ biochemically and structurally from those found between liver and myocardial cells. SDS PAGE and preliminary sequence data have as yet revealed little homology between principal polypeptides from enriched fractions of liver and lens-fiber gap junctions, even within the same species (9, 12, 16, 17, 27). Similarly, gel patterns of enriched myocardial gap junctions also appear unique (19). The junctions in these different tissues also may be distinguished in freeze-fracture replicas by their connexon (subunit) packing. For example, linear connexon aggregations are observed in fixed and unfixed freeze-fractured junctional plaques in myocardium (2, 7) but not in lens (12) or liver (30). There are dramatic interspecies differences in myocardial gap-junction structure as well (18). These differences may have functional counterparts reflecting metabolic or regulatory differences between different cell types, but this comparison has not yet been experimentally explored.

A gap junction with a particularly unusual structure is found joining lens-fiber cells. Lens-fiber junctions are so large and numerous that they cover a large fraction of the surface membrane (21). The biology of the lens suggests that lens-fiber gap junctions may have unique regulatory properties. Adult lenses are avascular and the lens fibers have little or no mitochondria, nuclei, or protein synthetic machinery (5, 6, 22). Thus, one would expect that lens-fiber gap junctions, unlike liver junctions (8, 37), are not turned over. Unlike liver and myocardial gap junctions, lens-fiber gap junctions exhibit a dispersed, disordered connexon array both *in situ* in fixed tissue and in vitro in isolated preparations obtained by subcellular fractionation (12). Recent reports indicate that connexons in isolated lens junctions may be crystallized into unusual hexagonal and square arrays by altering ionic conditions (28, 29); however, others have questioned these images (12, 20).

The meaning of crystallization or condensation of gap-junction connexons in any tissue is not known. Raviola et al. (30) studied the time-course of connexon condensation in rabbit ciliary epithelium using rapid-freezing technology and concluded that this structural change was too slow to be directly related to the physiological change from low to high resistance of the intercellular channels. Connexon condensation may therefore be a secondary consequence of the change to high resistance, such as increased junctional turnover (8). The observation that the lens-fiber connexons do not show this structural condensation, taken together with the unusual biology of the lens, prompted the hypothesis that communication between lens fibers may be resistant to some of the conditions which uncouple other cells (12).

We tested this hypothesis by studying the structure and regulation of gap junctions in embryonic-chick lens cells. It is known (30) that glutaraldehyde fixation facilitates the condensation or crystallization of connexons in gap junctions in some tissues but not in others, although the physiological meaning of this structural change is not known as reviewed above (12, 30). Using freeze-fracture replicas, we show that developing lens cells first express gap junctions whose connexons are condensed following aldehyde fixation. A few hours later in

THE JOURNAL OF CELL BIOLOGY · VOLUME 92 MARCH 1982 694-705

development, these cells then express gap junctions whose connexons are both condensed and dispersed. Having determined when dispersed connexons first appear during development, we then compare the ion and dye communication properties of lenses immediately before and after this junctional change. Turin and Warner (32, 33) have shown that lowering intracellular pH with elevated pCO_2 reversibly blocks electrical coupling between amphibian blastomeres, and Spray et al. (35) have shown this uncoupling to be "a simple and sensitive function of intracellular pH." We report here that, in embryonic chick lenses, elevated pCO_2 reversibly blocks dye transfer only between young lens cells which are joined by gap junctions with condensed connexon assemblies; intercellular dye movement between lens cells joined by gap junctions with dispersed connexon assemblies is not reversibly sensitive to elevated pCO_2.

MATERIALS AND METHODS

Fertilized, unincubated leghorn chicken eggs were obtained from Spafas, Inc. (Norwich, CT). Eggs were incubated at 37°C for 2–4 d before use. Embryos were carefully excised from the eggs, rinsed in Eagle's minimal Essential Medium (Gibco Laboratories, Grand Island Biological Co., Grand Island, NY) equilibrated with 95% O_2/5% CO_2, and staged according to Hamburger and Hamilton (14).

Scanning Electron Microscopy

Embryos were fixed for 1 to 24 h in 2.5% glutaraldehyde in 0.1 M sodium cacodylate buffer (pH 7.4). The embryos were rinsed several times in buffer, and the heads were removed and bisected in the mid-saggital plane with iris scissors. In some cases, the heads were further dissected with small fragments of a razor blade. The tissue was postfixed in 2% OsO_4 in H_2O for 1 h at 4°C, dehydrated in a graded series of alcohols, and dried in a Balzers (Lichtenstein) critical-point drier with CO_2 as the transition fluid. The embryo heads were mounted on aluminum stubs, sputter-coated with gold, and examined in a JEOL JSM-35 scanning electron microscope. A total of 32 embryonic lenses (stages 12–22) were examined.

Freeze-fracture

Embryo heads from all stages studied were removed, bisected in the midsaggital plane, and fixed for 20 min in 2% glutaraldehyde plus 2% formaldehyde in 0.1 M sodium cacodylate buffer (pH 7.4) supplemented with 0.5 mg/ml $CaCl_2$. The tissue was rinsed in buffer and the lenses were excised. In stage-12 to -13+ embryos, in which lenses were merely placodes, the whole hemisected heads were used for freeze-fracture. Following fixation and rinse, all specimens were incubated in 20% glycerol in 0.1 M sodium cacodylate buffer for 1–2 h, and each lens was placed on a gold hat in a drop of glycerol-buffer and frozen in liquid Freon-22 cooled to −150°C with liquid nitrogen. Lenses were fractured *in vacuo* at −115°C and shadowed with platinum-carbon in a Balzers BAF301 freeze-etch machine. Replicas were cleaned in methanol followed by Clorox-KOH, rinsed in H_2O, picked up on Formvar-coated grids, and examined in a Siemens 101 electron microscope. Replicas of 44 fractured embryonic lenses (stages 12–22) were examined and photographed. Some of these lenses were first used in dye transfer experiments (see below) before fixation. It must be emphasized here that we correlated the sensitivity of intercellular dye transfer to elevated pCO_2 with the freeze-fracture appearance of aldehyde-fixed junctions. We did not attempt to rapid-freeze physiological specimens. Specimens from all ages were fixed under identical conditions.

The criteria used to determine whether a connexon assembly was condensed or dispersed are as follows. For condensed assemblies, connexons were separated from each other by a maximum of 10 nm and displayed obvious crystalline arrays of pits on the E fracture-face (see Fig. 2 *a*). For dispersed assemblies, connexons were separated by a minimum of 15 nm and showed no obvious long-range order. Our analysis of connexon condensation was limited by necessity to only those particle arrays which were large enough to show the characteristics of gap junctions. Clearly, there may well have been minute aggregations of connexons or single connexons which could not be identified in freeze-fracture replicas and which therefore could not be included in this analysis. The unique morphology of the dispersed gap-junction connexons aided in distinguishing them from the rare aggregations of other intramembrane particles. As seen in Fig. 2, the connexons are homogeneous in size and appear larger and more distinct than other intramembrane particles. In the membrane, the connexons occupy a domain by themselves and exclude the heterogeneously-sized nonjunctional particles. In areas with appropriate fracture planes, the connexon domains occupy areas of close membrane apposition and reveal clear E-face pits on the reciprocal fracture-face.

Electrical Coupling

After being staged, embryos were decapitated and the heads were bisected in the midsaggital plane. Each hemisected head was pinned ectoderm-side-down on a layer of Sylgard (Dow Corning Corp. Midland, MI) overlying the glass cover slip bottom of a Plexiglas chamber. The brain and optic cup (or optic vesicle) were dissected away, exposing the posterior surface of the developing lens. Care was taken to avoid touching or damaging the lens surface. Fig. 3 *a* and *b* are scanning electron micrographs of a chick head dissected in this way. For embryos younger than stage 14−, when the lens was still a thickened placode, only the posterior half of the optic vesicle was removed, leaving the anterior half (adjacent to the lens) *in situ*. The half-head was turned over and pinned in place with the ectoderm up. In these early embryos, attempting to remove the entire optic vesicle resulted in lens damage and poor resting potentials.

The chamber was placed on the stage of a Zeiss IM-35 inverted microscope equipped with Normarski differential interference contrast optics and fluorescence epi-illumination optics. The entire stage was warmed to 30°C with an infrared lamp. A stream of 95% O_2/5% CO_2 was directed over the preparation throughout the experiment.

Paired intracellular recordings were made using high resistance (80–120 MΩ) microelectrodes filled with 3 M KCl. Electrodes were positioned with micromanipulators and connected to electrometers equipped with active bridge circuits. Current pulses were recorded directly with a virtual ground circuit.

Electrical coupling was studied by passing an 0.5 to 1-s, 0.5- to 3-nA current pulse through one intracellular electrode and recording the potential change in a cell 20–150 μm distant with the second electrode. Then the roles of the electrodes were reversed. In both cases, several trials were performed in which the pulse polarity was reversed and pulse amplitude varied. In principle, one can monitor membrane potential and inject current into the same cell at the same time with an active bridge circuit. In these experiments, however, the high-resistance electrodes were non-ohmic in the nA current range, making it impossible to balance the bridge. With lower resistance electrodes, it was possible to balance the bridge but impossible to obtain stable penetrations. Therefore, we were unable to determine coupling ratios (i.e., the ratio of induced voltages in the two cells).

The steady state magnitude of current pulses and voltage responses, and the time-course of rising and falling phases of voltage responses, were determined from high-speed (10 cm/s) strip-chart records and from oscilloscope traces.

Dye Transfer

Intercellular dye transfer was studied by iontophoresing a fluorescent tracer into a lens cell and following dye movement into surrounding cells in real time with epi-illumination fluorescence optics. Micropipettes were pulled as described above. The electrodes were filled from shoulder to tip with a 4% solution of Lucifer yellow CH (the generous gift of W. Stewart) or in a few cases with uranine (the disodium salt of fluorescein; Sigma Chemical Co., St. Louis, MO) in water. The micropipette barrels were subsequently back-filled with an 0.1% LiCl solution. Recordings and current injections with dye-filled microelectrodes were done as described above, except that only one electrode was used at a time. Dye was injected by passing 0.5-s, 3-nA current pulses at 1 Hz. Current polarity was alternated every cycle to minimize tip blockage. During most of each experiment, fluorescence illumination was off; it was turned on from time to time to monitor the injection and subsequent dye movement and to take photomicrographs. All photos were taken on 35-mm Tri-X film exposed at ASA 800. In some experiments, lenses were fixed 1–5 min after dye injection, cleared, and whole-mounted for additional micrographs (see Light Microscopy, below). Fixation took place for 20 min to several hours in 4% paraformaldehyde in 0.1 M sodium cacodylate buffer (pH 7.4).

Horseradish Peroxidase Injections

One or two cells in each of several lenses were injected with horseradish peroxidase (HRP). Micropipettes were filled with a 2% solution of HRP (Boehringer Mannheim Biochemicals, Indianapolis, IN) in 0.2 M potassium acetate (pH 7.2). After each cell was impaled, current pluses (50 ms, 3 nA) of alternating polarity were delivered at 20 Hz for 1–5 min. The lens was then fixed for 60 min in 1% glutaraldehyde in 0.1 M sodium cacodylate buffer (pH 7.4) at room temperature.

After two buffer rinses, the HRP reaction was run according to Graham and Karnovsky (13) with the modification of Malmgren and Olsson (25). Before the

reaction, the specimens were rinsed two times in Tris buffer (pH 7.4), then incubated in 0.5% cobalt chloride in Tris buffer for 10 min (1). Specimens were then rinsed once each in Tris buffer, then phosphate buffer (pH 7.4). The diaminobenzidine (DAB) reaction was carried out in the dark in cacodylate buffer (pH 5.1) with 2 mg/ml DAB and 0.1% H_2O_2, followed by three rinses in phosphate. Specimens were whole mounted, without osmication, as described below.

Fluorescein Isothiocyanate-Insulin Injections

100 mg of lyophilized bovine insulin (Sigma Chemical Co.) was reconstituted in 10 ml of carbonate buffer (0.025 M Na_2CO_3, 0.025 M $NaHCO_3$, pH 9.8). The solution was placed in a dialysis bag (Spectra Por 3, 3,500-mol wt cutoff; Fisher Scientific Co., Pittsburgh, PA) and incubated for 24 h at 4°C in 100 ml of 0.01% fluorescein isothiocyanate (FITC; Sigma Chemical Co.) in carbonate buffer. The bag was then placed in phosphate-buffered saline, which was changed twice daily until the OD 480 of the dialysate vs. fresh saline was zero (4 days). The FITC-insulin was prepared by Dr. Roberta Pollock (Harvard Medical School).

Microelectrodes were filled with the dialyzed FITC-insulin, and lens cells were given intracellular tracer injections as described above for HRP. Lenses were fixed for 30–90 min in 2% paraformaldehyde in 0.1 M sodium cacodylate buffer (pH 7.4) and subsequently processed for light microscopy.

Light Microscopy

Some of the lenses injected with Lucifer yellow, and all of those injected with HRP and FITC-insulin, were cleared for photomicroscopy. Each fixed lens was rinsed in 0.1 M sodium cacodylate (pH 7.4) and dehydrated in a graded series of ethanol. Lenses were transferred from 100% ethanol to xylene, and then placed on a microscope slide in a drop of Lustrex HF555 plastic (Monsanto Research Corp., Monsanto Co., Dayton, OH) dissolved in xylene. A cover slip, supported by spacers, was placed over the tissue. Micrographs were taken on Tri-X film exposed at ASA 800.

Embedding and Sectioning

After fixation, the lenses were rinsed in buffer and dehydrated in an ethanol series. Lenses were embedded in JB4 embedding medium (Polysciences, Inc., Warrington, PA) according to supplied directions. Serial sections (6 μm each) were cut through the lens, placed on glass slides, flattened by exposure to water droplets, dried, and photographed on a Zeiss Photoscope with Tri-X film.

Bath Solutions

When not stated otherwise, embryos used in physiology experiments were incubated in Eagle's minimal essential medium with Earle's salts equilibrated with 95% O_2/5% CO_2 (pH 7.2–7.25). In CO_2 uncoupling experiments, the medium was equilibrated with 60% O_2/40% CO_2 (which lowered pH to 6.35), 50% O_2/50% CO_2 (pH 6.20), 40% O_2/60% CO_2 (pH 6.10), 20% O_2/80% CO_2 (pH 6.00), or 100% CO_2 (pH 5.95).

In acetate buffer uncoupling experiments, embryos were bathed in modified Earle's salts solution in which NaCl (normal concentration of 116 mM) was replaced by sodium acetate (91 mM) and the solution was buffered either to pH 6.8 with 25 mM HEPES (Sigma Chemical Co.), to pH 6.4 with 25 mM PIPES (Sigma Chemical Co.), or to pH 6.0 with 25 mM MES (Sigma Chemical Co.). In parallel control experiments, embryos were bathed in modified Earle's salt solution in which the NaCl concentration was lowered from 116 mM to 91 mM and the solution was buffered either to pH 6.4 with 25 mM PIPES or to pH 6.0 with 25 mM MES.

RESULTS

After glutaraldehyde fixation, the subunits (connexons) of gap junctions in many tissues appear condensed and crystalline, but connexons joining mature lens fibers (12) appear dispersed and noncrystalline. Here we examine developing chick lenses morphologically to define the stage at which dispersed connexons are first detectable, and then we compare the ion- and dye-transfer properties of lens cells before and after this morphological change.

Morphology of Developing Lenses

In stage-12 to -13 chick embryos, the optic vesicles grow out from the neural tube and each induces the overlying ectoderm to thicken, forming the lens placodes (reviewed in Hamilton [15]). The placode appears as a raised plate in Fig. 1 *a*. Beginning at about stage 14−, the lens placode invaginates, forming the lens vesicle, as the optic vesicle folds inward to form the optic cup. Viewed from the outside, this invagination produces a pore in the head (Fig. 1 *b*) that joins the lumen of the lens vesicle with the extraembryonic space. By cutting away the head ectoderm, one can see the lens vesicle lying behind the lens pore in the optic cup (Fig. 1 *c*). During stage 15, the lens pore narrows (Fig. 1 *d*) and eventually closes, and by stage 17 to 18− the lens vesicle is a hollow cyst pinched off from the overlying ectoderm (Fig. 1 *e*). The posterior cells of the lens vesicle then elongate, extending into the lumen. By stage 19+ to 20, they meet the anterior cells (Fig. 1*f*), thus establishing the first lens fibers.

Gap Junctions in Developing Lenses

During formation of the lens placode and the initial stages of placode invagination (stages 12 to 14−), freeze-fracture replicas of aldehyde-fixed lenses reveal gap junctions with a condensed connexon morphology. The junctions are relatively small and infrequent at these early stages, and they always show regular arrays of connexons on the membrane fracture faces (Fig. 2 *a*). By stage 14+ to 15−, small gap junctions are found that have a mixed connexon packing: islands of condensed connexons exist within larger assemblies of dispersed connexons (Fig. 2 *b*). During the next several stages, gap junctions with mixed connexon assemblies increase in size and number (Fig. 2 *c*, *d*, and *e*). The mixed packing can be seen on both the P- and E-fracture faces (Fig. 2 *c* and *d*). By stage 22, one can occasionally find junctions with only dispersed connexon assemblies, as in adults (data not shown). In addition, junctions with only condensed connexons can be found at any stage from 12 to 22.

Despite this heterogeneity of gap-junction morphology in embryonic lenses, it appears that stage 14 is a critical period in gap-junction expression: younger embryonic lenses contain only condensed connexon assmblies, but lenses in older embryos contain both condensed and dispersed connexon assemblies. Thus, there is a critical period of about 3 h which can be probed experimentally.

FIGURE 1 Scanning electron micrographs of embryonic chick lenses. Each bar represents 0.1 mm. (*a*) The left half of a stage-13 chick head. Note the lens placode (*pl*). × 30. (*b*) A stage 14 chick head. The placode has invaginated, creating the lens pore (*lp*) (arrow). × 70. (*c*) Side view of a stage-14 lens. The head was cut perpendicular to the surface and lateral to the lens pore, exposing the underlying lens vesicle (*lv*) and the optic cup (*oc*). Part of the optic cup was cut away. × 510. (*d*) Top view of a stage 16− lens vesicle. Part of the ectoderm was removed, and in the process the optic cup was also cut. Note the small size of the lens pore. × 250. (*e*) Side view of a bisected stage 17− lens vesicle. The cut was made perpendicular to the ectoderm surface. Invagination was complete. × 220. (*f*) Side view of a bisected stage 20 lens. The overlying ectoderm was removed. The posterior lens cells have elongated, obliterating the lumen of the lens vesicle. × 250.

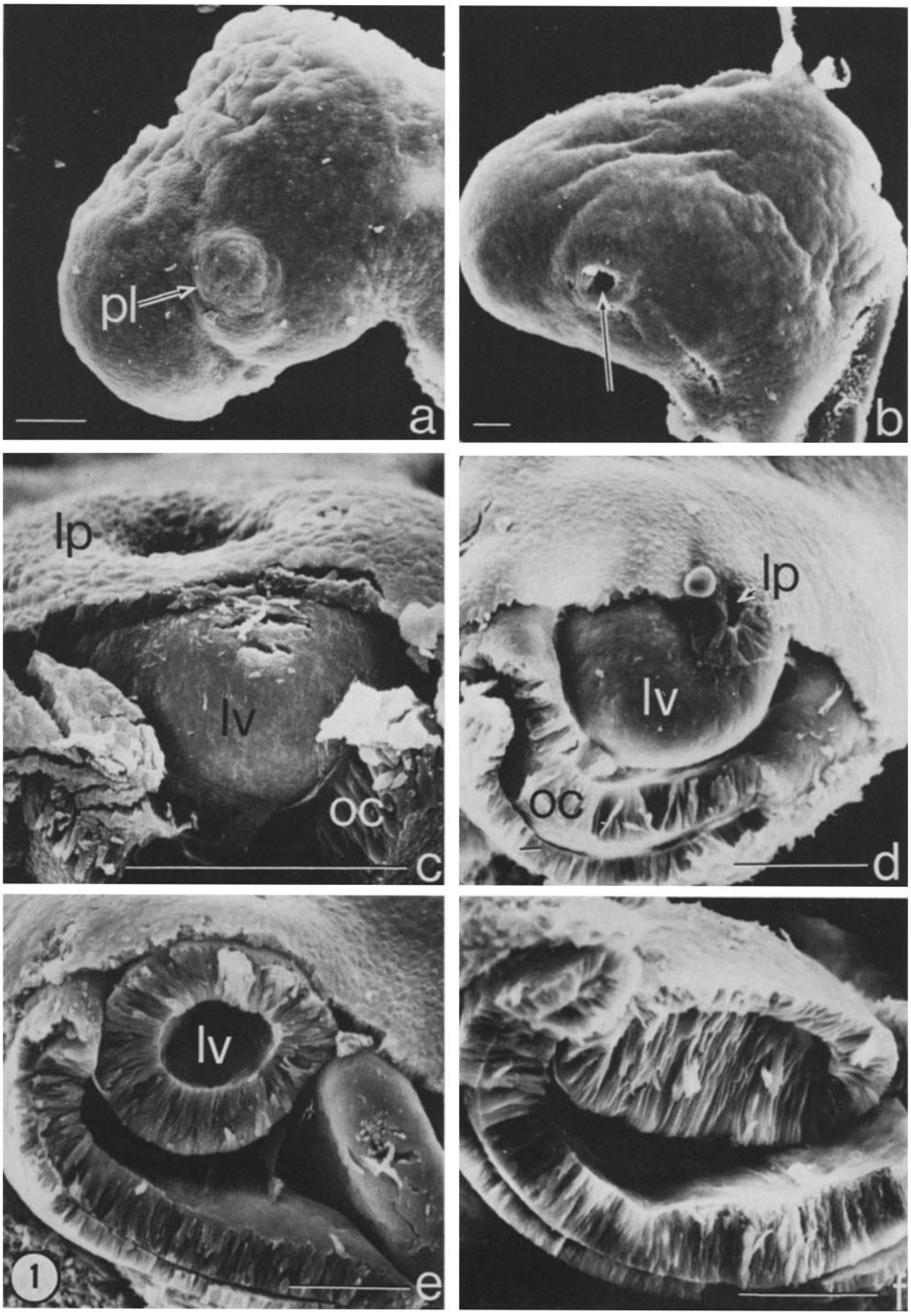
pl
a
b
lp
lv
oc
c
lp
lv
oc
d
lv
1
e
f

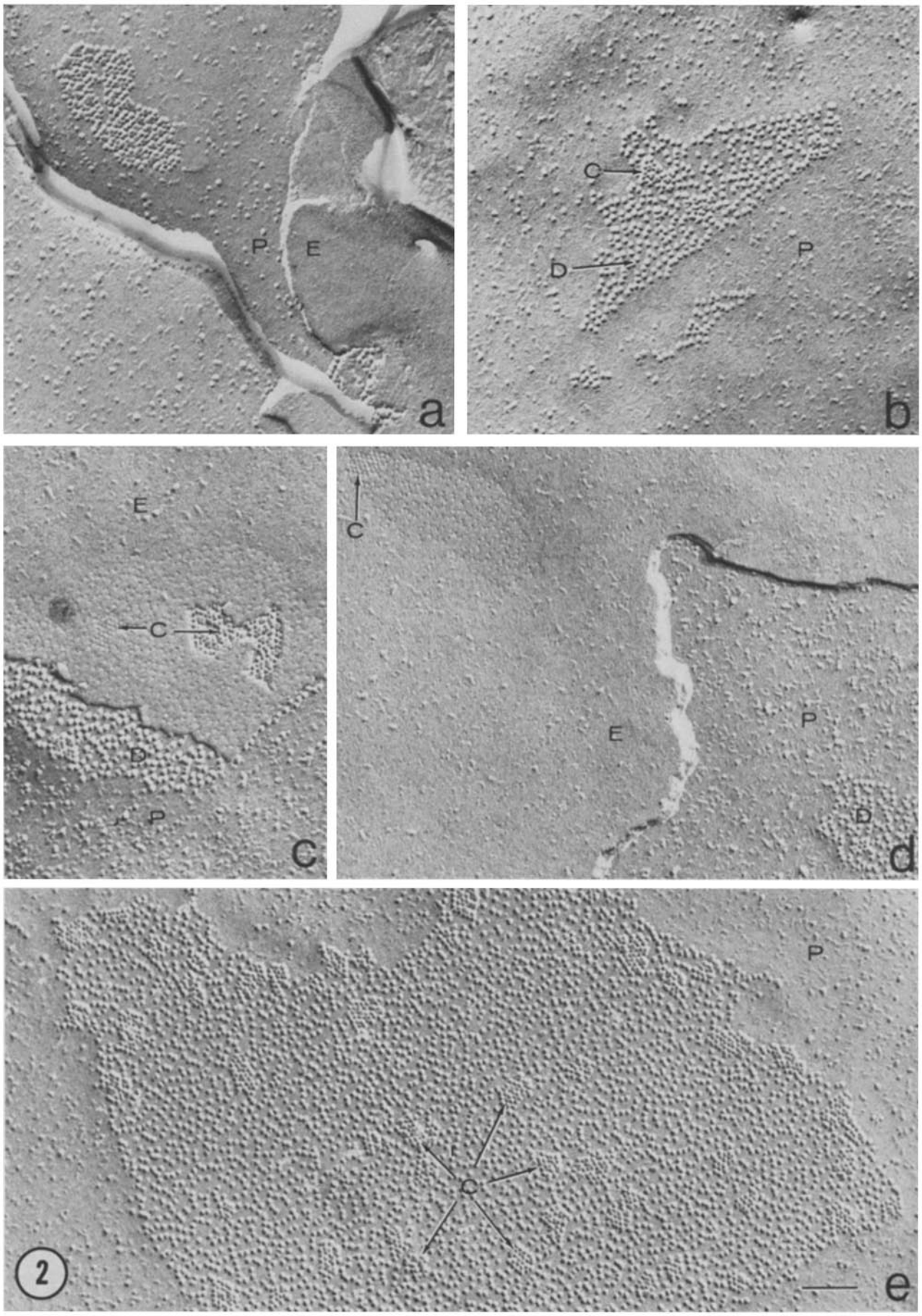
P
E
a
C
D
P
b
E
C
D
P
c
C
E
P
D
d
P
C
2
e

The absolute number of gap junctions joining the developing lens cells at different stages was not determined due to technical and theoretical difficulties. In younger lenses, we confined our observations to those cells which could be clearly identified as lens cells, using histological ciriteria. This severely limited our sample, since we examined mainly cross-fractured cells with minimal membrane fracture face area. Cells with large fracture faces generally could not be unequivocally identified as lens cells. In addition, freeze-fracturing is not a random process, and therefore standard morphometric techniques cannot be rigorously applied.

Electrical Coupling

Lmbryonic lens cells are electrically coupled at all stages from 13 to 22. In each lens studied (Fig. 3), high-resistance (80–120 MΩ) micropipeties were inserted into two cells 10–150 μm apart. Resting membrane potentials were −60 to −70 mV at all stages, though in the smaller, younger lenses it was more difficult to obtain stable penetrations. The potentials recorded by the two microelectrodes were usually within 5 mV of each other.

Injection of small (1–3 nA), 0.5-s current pulses through one micropipette evokes electrotonic potential changes at the site of the second micropipette (Fig. 4). Similar results are observed when the roles of the micropipettes are reversed. The steady state voltage shift is linearly related to current magnitude in any given lens, indicating the absence of rectification at the level of the current passed.

The strength of electrical coupling is usually expressed as the coupling ratio, defined as the ratio of the voltage shifts induced in the two cells. We cannot directly measure a coupling ratio because the electrodes required for stable penetrations are so small that they are non-ohmic during nA current injections, thus making it impossible to balance a bridge circuit.

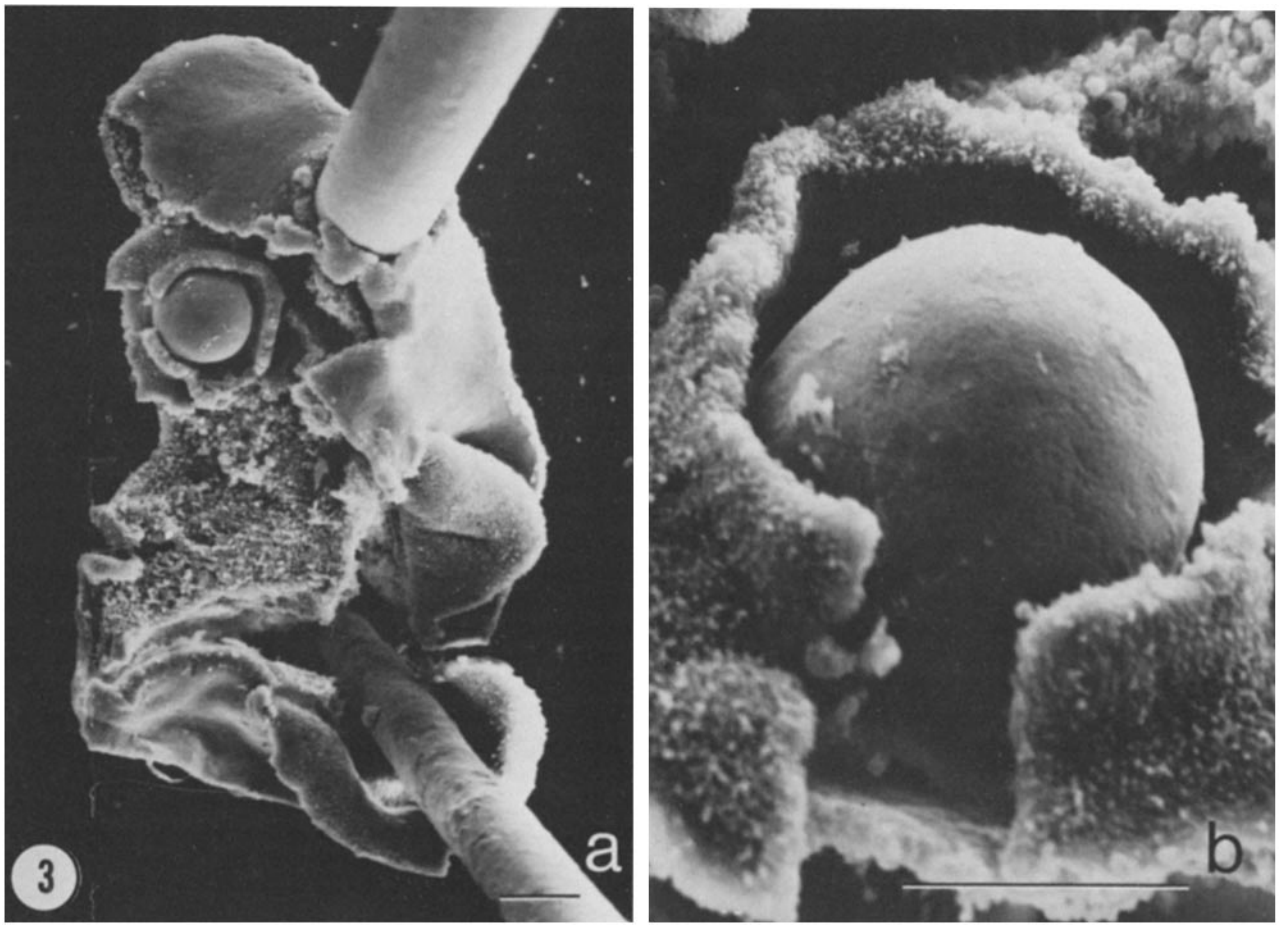

FIGURE 3 Scanning electron micrographs of a lens prepared for electrophysiology. (*a*) The right half of a stage-16 embryonic chick head dissected to expose the posterior lens surface. The large cylinders are insect pins. × 100. (*b*) Close-up view of the lens and the surrounding optic cup. × 380. Bars, 0.1 mm.

FIGURE 2 Freeze-fracture replicas of embryonic lens-cell gap junctions. (*a*) At stage 14, gap junctions are found which have only condensed connexon assemblies, seen as tight aggregates of particles and pits on the P and E fracture-faces. (*b*, *c*, and *d*) These micrographs of gap junctions between chick lens cells at stages 15, 16, and 17, respectively, reveal connexons arrayed in both condensed (*C*) and dispersed (*D*) assemblies within the same junctional plaques. (*e*) By stage 20, large gap junctions can be found between adjacent lens cells. These junctions still display the mixed condensed and dispersed morphology. *P*, protoplasmic membrane leaflet; *E*, external leaflet. Bar, 100 nm. × 100,000.

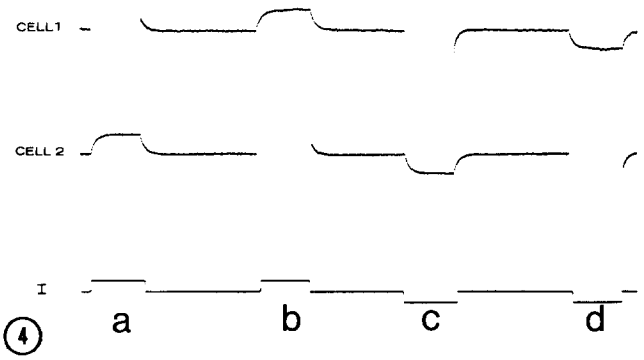

FIGURE 4 Electrical coupling in a stage-17 embryonic lens. (*c*) When a 1-s, 1-nA negative current pulse (*I*) is injected into one lens cell (*cell 1*), a 4.5-mV hyperpolarization is recorded in a second cell 20 μm distant (*cell 2*). (*d*) Injecting current into *cell 2* polarizes *cell 1*. (*a* and *b*) Depolarizing current pulses are equally effective.

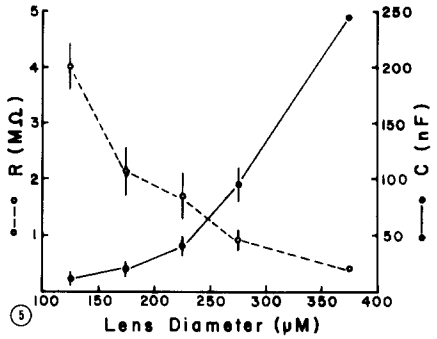

FIGURE 5 Input resistance (*R*) and input capacitance (*C*) of embryonic lenses as a function of lens diameter. Each point is the mean value from three to six lenses, except for the single values at 375 μm. Bars indicate ±1 SD.

Nevertheless, several observations demonstrate that coupling between embryonic lens cells is very tight. First, the recorded polarization is independent of the distance between the current injection site and the recording site. For example, injecting a 3-nA current pulse into one cell of a stage-16 lens induced the same 4.8–5.0 mV potential change in cells 17 μm, 60 μm, and 80 μm distant (the lens was ~200 μm in diameter). Second, the rising and falling phases of the electrotonic potential shifts are very nearly simple exponentials. Least squares regression of rising or falling phases to simple exponentials gives a mean correlation coefficient of 0.99 ± 0.005 (mean ± SD; $n = 11$ lenses). This indicates that embryonic lens cells are so well coupled that the entire organ comprises a single intracellular electrical compartment.

During development, the input resistance, R, decreases and the input capacitance, C, increases. These changes reflect the increasing size of the lens (Fig. 5). Beyond stage 14+, positive and negative current pulses (1–3 nA) induce polarizations of equal magnitudes. In stage-13 and -14 lenses, however, depolarizing currents induce potential changes 20% larger than do hyperpolarizing currents of equal size. Even in young lenses, R is independent of the distance between the electrodes, indicating that junctional membrane resistance is low compared to that of nonjuctional membrane. Therefore, the rectification observed in stage 13–14 lenses must reflect voltage-dependent properties of nonjuctional membrane. These experiments give no evidence for developmental changes in the electrical properties of junctional membrane. On the other hand, our approach would not readily detect such differences if they did exist.

Dye Transfer

Cell communication is also studied by injecting lens cells with a fluorescent dye and monitoring dye movement. A cell is impaled with a micropipette filled with 4% Lucifer yellow, and dye is iontophoresed into the cell with 3 nA, hyperpolarizing current pluses. Resting potentials measured with Lucifer yellow-filled electrodes are −60 to −70 mV, as before. It is possible to monitor dye injections and dye movement in real time by observing the lens with fluorescence optics.

Soon after Lucifer yellow is injected into one cell, the dye is found in dozens of surrounding cells (Fig. 6). The dye spreads so quickly that it is generally impossible to temporally separate filling of the impaled cell from dye movement into adjacent cells. In particular, we can not freeze the first stages of dye movement photographically because there is considerable dye spread over the time-course of a single exposure (usually 4 s). An example of the later stages of dye movement is shown in Fig. 6*b–d*. At the end of a 30-s injection, Lucifer yellow is already present in many cells. Over the next minute, the diameter of the cloud of fluorescence expands about twofold. After 6 min, the dye has diffused so much that fluorescence is below detectability in most of the lens. With sufficiently long injections, however, it is possible to make the entire lens fluorescent. Similar results are obtained when the disodium salt of fluorescein (uranine) is substituted for Lucifer yellow.

Dye moves via an intracellular pathway. When the Lucifer yellow-filled micropipette is advanced slightly, so that the resting potential is lost and the tip is presumably extracellular, dye injection does not stain lens cells. More direct evidence is obtained by fixing, embedding, and sectioning dye-filled lenses. It is clear from the stained nuclei in the sections that Lucifer yellow is intracellular (Fig. 6*e–g*).

FIGURE 6 Dye transfer in the lens (*a*) A stage-14 lens that was given an intracellular injection of Lucifer yellow and fixed several minutes later. The dye stains ~50 cells surrounding the injection site. Simultaneous Normarski and fluorescence optics. × 200. (*b*, 334*c*, and *d*) Time-course of dye spread in a living stage 20 lens. A single cell was given a 30-s injection of Lucifer yellow and photographed with fluorescence optics 10 s (*b*), 1 min (*c*), and 6 min (*d*) after the injection. × 200. (*e*, *f*, and *g*) Sections of dye-filled lenses. Each lens was given a single intracellular injection of Lucifer yellow and then fixed, embedded, sectioned, and photographed with fluorescence optics. (*e*) Stage 13− (cf. Fig. 1 *a*). × 400. (*f*) Stage 13+ (cf. Fig. 1 *b*). × 380. (*g*) Stage 16− (cf. Fig. 1 *e*). × 240. Bars, 50 μm.

FIGURE 7 Lens whole-mounts with cells filled with HRP. One or two cells in each lens were injected with HRP, and then the lenses were fixed and histochemically stained. Bars, 25 μm. (*a*) Stage 14. × 480. (*b*) Stage 15. × 480. (*c*) Stage 16+ (the lower stained cell is viewed end on). × 680.

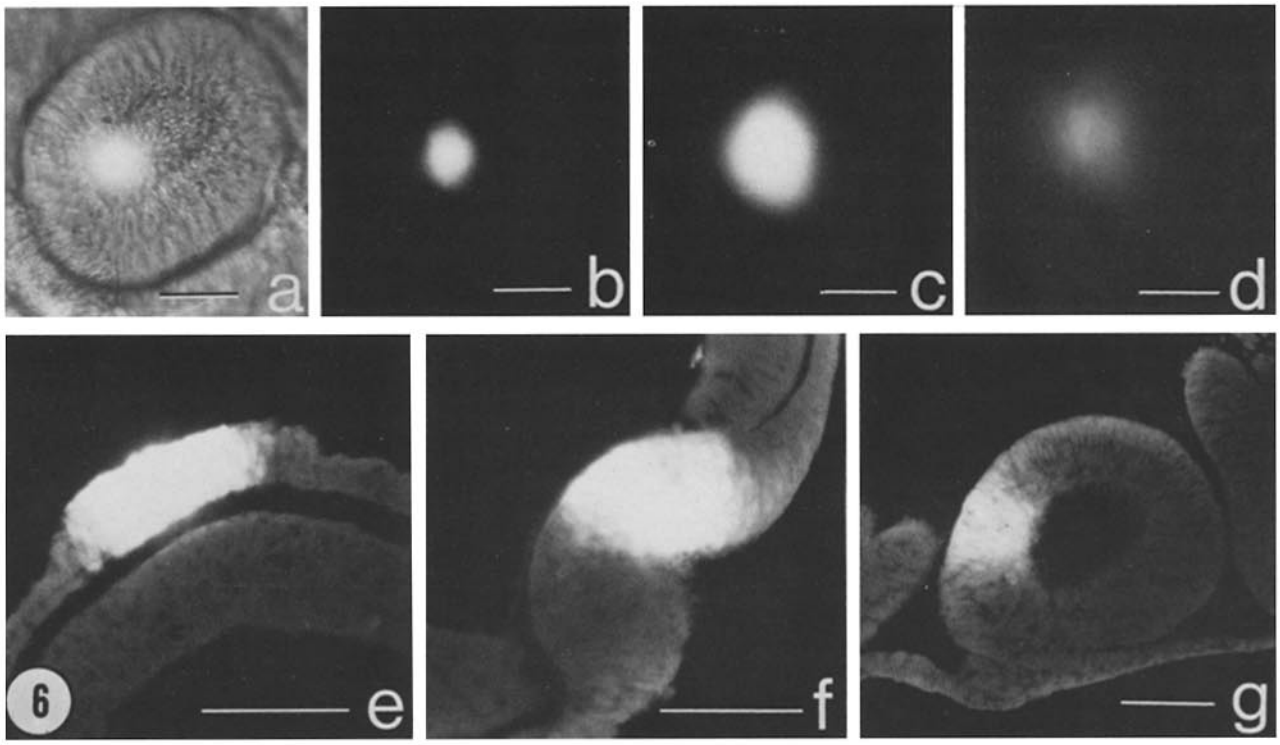
a
b
c
d
6
e
f
g

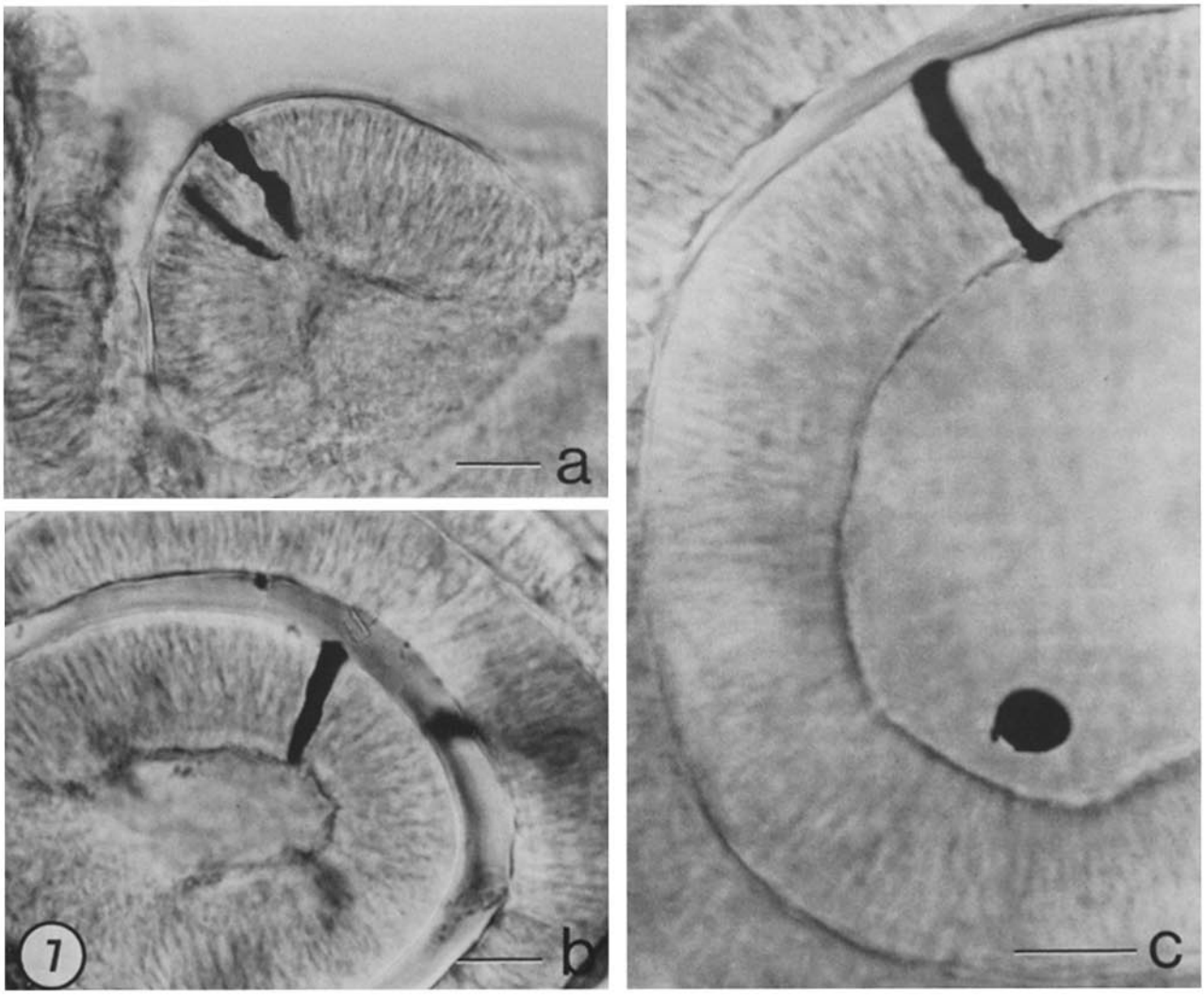
a
7
b
c

At all developmental stages beyond stage 14, the apparent rate of dye movement is similar in all lenses. In most stage-12 and -13 lenses, however, dye movement is strikingly slower. Lucifer yellow often fills the impaled cell completely before there is detectable fluorescence in neighboring cells. Dye movement in these young lenses is first noticeable as a loss of sharpness of the impaled cell's boundary. This slow movement may be due to the small size and sparse number of gap junctions in young lenses (cf. Fig. 2*a*). On the other hand, the rate of dye movement is not correlated with the connexon arrangement in junctions in freeze-fracture replicas. In stage-14 lenses, dye movement is rapid, yet connexons are aggregated in the same way as in younger lenses.

Electrical Coupling and Dye Transfer Occur Via Gap Junctions

It is important in measuring communication between rapidly dividing cell populations to rule out coupling via patent intercellular bridges due to incomplete cytokinesis. We therefore injected lens cells with HRP and FITC-insulin, molecules which would be expected to move through intercellular bridges (23) but not through gap junctions (10, 11, 34). The HRP data are shown in Fig. 7*a-c*, which are photographs of whole-mounts of the embryo preparations after HRP injections and localization, as detailed in the Materials and Methods.

In Fig. 7*a*, two cells in an early stage-14 embryo lens were individually injected with HRP. Fig. 7*b* shows an HRP-injected cell in a stage-15 embryo, and Fig. 7*c* shows a pair of cells (one viewed from above, the other in profile) in a stage-16 embryo. In all cases, and in all cases of cells injected with FITC-insulin (data not shown), the injected molecules were confined to single cells, demonstrating the lack of any network of intercellular bridges joining the cells. This was also evident in sections of lenses with HRP-filled cells (not shown). Thus, we conclude that both electrotonic and dye coupling occur via gap junctions and not by intercellular bridge routes.

CO_2-Mediated Uncoupling

Replacing normal medium with medium equilibrated with at least 50% CO_2 effects a loss of dye transfer in stage-12 to -14 embryos. After lenses are bathed in the 50% CO_2 medium for at least 10 min, intracellularly injected Lucifer yellow is confined to single cells. The minimum exposure time for CO_2 to effect uncoupling varies from lens to lens, but it is not correlated with the age or size of the lens. Fig. 8*a* and *b* and show paired Nomarski and fluorescence photomicrographs of a stage 14– embryo that was exposed to 50% CO_2 medium for 15 min before receiving two intracellular injections of Lucifer yellow. No dye spread was observed during the next 5 min, after which the lens was fixed with formaldehyde, cleared, and photographed. The 50% CO_2 level appears to be near threshold. 40% CO_2 was found to be ineffective in three cases in which 50% CO_2 subsequently induced loss of dye transfer.

CO_2-mediated uncoupling in young lenses is reversible. In experiments, the medium was changed back to medium equilibrated with 5% CO_2. 10–15 min later, injecting single cells with Lucifer yellow produced clouds of fluorescence in 11 cases, as in untreated lenses (cf. Fig. 6*a-d*). In the three other cases, there was no recovery of dye transfer. Apparently, these lenses were killed by CO_2: the resting potentials in these lenses decreased to zero and remained there. It is not clear why these lenses were particularly sensitive to CO_2 but, as noted above, lenses also vary in their susceptibility to the onset of CO_2-mediated uncoupling.

Out of 23 experiments performed on embryos at stage 14+ or younger, uncoupling was seen in 18 cases. The five lenses resistant to CO_2 were stage 14 to 14+, and they were the five largest. This indicates that sensitivity to CO_2-mediated uncoupling is lost late in stage 14. In fact, no uncoupling by 50–80% CO_2 was seen in any lens from embryos older than stage 14+ ($n = 8$ lenses). An example is shown in Fig. 8*c-d*. 20 min after a stage-15 embryonic lenses is incubated in 80% CO_2 medium, there is no detectable change in the pattern of dye spread compared to untreated controls. Older lenses are even resistant to 100% CO_2 unless the treatment is prolonged (see below).

Comparison of these results with the freeze-fracture data reveals a close correlation between CO_2 sensitivity and the morphology of the connexon assemblies after fixation with aldehydes. If dye transfer is blocked between the lens cells by elevated pCO_2, then the gap junctions always have condensed connexon assemblies. If the cells are resistant to this CO_2 effect, freeze-fractured gap junctions display the mixed morphology: a mosaic of both condensed and dispersed connexons, usually within the same junctional plaque.

It should be noted that even in stage-13 to -14 embryos, elevated pCO_2 does not abolish electrotonic coupling. This was especially clear in one experiment in which a stage-13+ embryonic lens was impaled with one KCl-filled electrode and one Lucifer yellow–filled electrode. Passing current through the Lucifier yellow-filled pipette stained only a single cell, but a potential change was recorded with the KCl-filled electrode during the dye passing current pulses. Interpretation of this phenomenon is complicated by the multiple effects of high pCO_2 on the electrical properties of the lens. Raising the CO_2 level to 50% decreases the resting potential from −70 mV to ~−20 mV. In addition, the input resistance, R, measured as defined above, increases by up to fourfold, though the size of the increase in highly variable (cf. reference 33). This increase in R reflects an increase in the resistance of nonjunctional membrane, which obscures any concomitant change in junctional resistance. Thus, we cannot dissect what effects the elevated pCO_2 has on junctional membranes. The observation that high pCO_2 blocks dye coupling but not electrical coupling may imply either that all junctional channels close part way or that a small subpopulation of channels remains open.

CO_2-Mediated Block of Dye Transfer Is a Function of Intracellular pH

Several experiments indicate that uncoupling of young lenses by high pCO_2 is due to a decrease in intracellular pH. Three

FIGURE 8 Developmental loss of CO_2-induced blockage of dye transfer. (*a* and *b*) A stage 14 lens that was preincubated for 15 min in medium equilibrated with 50% CO_2/50% O_2 and given two intracellular injections of Lucifer yellow. The dye is confined within the injected cells, demonstrating blocked dye transfer. Paired Nomarsky and fluorescence micrographs. × 560. (*c* and *d*) A stage-15 lens that was preincubated for 20 min in medium equilibrated with 80% CO_2/20% O_2 and given a single intracellular injection of Lucifer yellow. The dye spreads freely, indicating no detectable uncoupling. *LP*, lens pore. × 600. Bars, 25 μm.

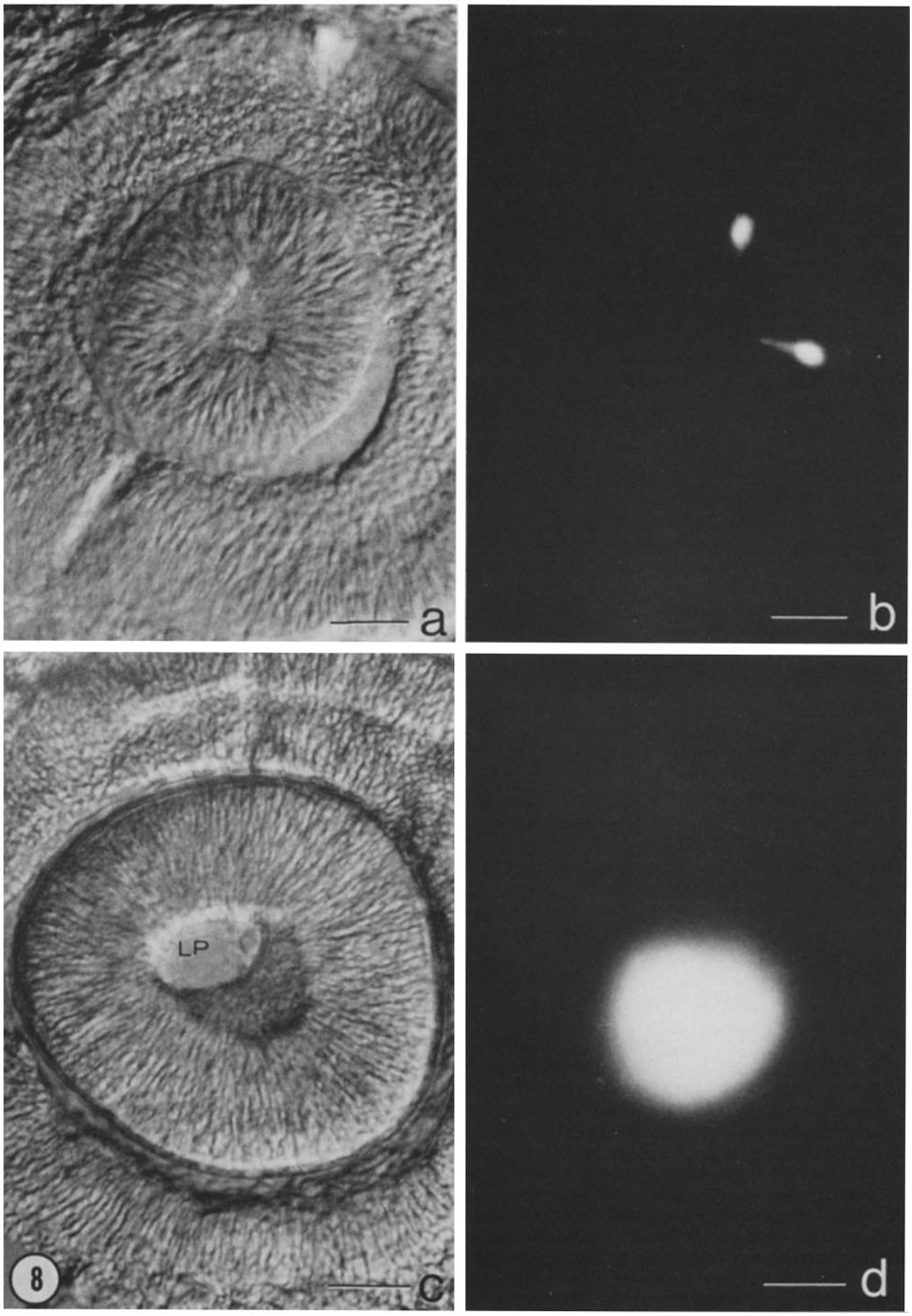
a
b
LP
8
c
d

stage 14− to 14 embryos were incubated in media in which NaCl was replaced with Na-acetate and HEPES buffer (pH 6.8–7.0, see Materials and Methods) (3). Acetate ions lower intracellular pH because they may combine with protons, cross the membrane, and release the protons intracellularly. After 40-min incubation in oxygenated acetate buffer, all three lenses showed reversible blockage of dye transfer, just as in the CO_2 experiments.

Neither anoxia nor extracellular pH changes can reproduce the CO_2-mediated block of dye transfer. In two experiments, cells in stage 14− lenses continued to transfer dye after 40-min exposure to normal medium equilibrated with 100% N_2. In three experiments, lowering the extracellular pH to 6.0 with 2,(*N*-morpholino)ethane sulfonic acid (MES), an ion that does not cross cell membranes, did not block dye transfer in stage 14− lenses. Taken together, these experiments implicate lowered intracellular pH as a trigger for blocking dye transfer.

Uncoupling of Older Lenses (Stages 15− to 22)

Several procedures will block dye transfer in older lenses with dispersed junctional connexons. Each of these procedures results in cell death, as defined by an irreversible loss of resting potential. Ten of thirteen older lenses exposed to 100% CO_2 eventually uncoupled. In five cases, the detectable block of dye transfer was complete. In the other five cases, intracellular injection of Lucifer yellow initially filled single cells, but the dye slowly spread to neighboring cells over the next several minutes. At least 25–35 min of exposure of 100% CO_2 was required for dye blockage. When these uncoupled lenses were reincubated in medium with 5% CO_2/95% O_2, coupling was not restored and resting potentials did not recover. There was one exception, however, in which a stage-16 lens uncoupled after 7 min in 100% CO_2 and recovered several minutes after the CO_2 level was lowered to 5%. We have not been able to repeat this observation, however.

Acetate-rich medium buffered with HEPES to pH 6.8–7.0, which uncouples young lenses, is ineffective in reducing dye transfer in older lenses. On the other hand, acetate medium buffered to pH 6.4 with PIPES drives the resting potential to zero and irreversibly blocks dye transfer between the cells (two experiments). In three other experiments, exposure of the lenses to low levels (<0.1%) of either glutaraldehyde or formaldehyde rapidly and irreversibly blocks dye transfer between the cells. In summary, the only conditions we have found that uncoupled lenses beyond state 15− do so irreversibly (with the one exception) and also effect cell death.

DISCUSSION

This work demonstrates a close temporal correlation between the expression of lens fiber-specific gap junctions and the loss of sensitivity to CO_2 with respect to dye transfer. Up to embryonic stage 14, freeze-fracture replicas reveal that chick lens cells are joined by gap junctions which have exclusively condensed connexon assemblies. Lenses at these stages are reversibly uncoupled by 10- to 30-min exposure to medium gassed with 50% CO_2. Beyond embryonic stage 14, fixed chick lens cells are joined by gap junctions with both condensed and dispersed connexon assemblies. Dispersed assemblies are characteristic of gap junctions between adult lens fibers. Coincident with this change in junction morphology, developing lenses become resistant to CO_2-induced blockage of dye transfer.

Dye transfer in older embryonic lenses can be blocked experimentally. In our experience, with the one exception noted in Results, blockage of dye transfer in lenses with dispersed connexons is irreversible and is accompanied by a complete loss of resting potentials. The physiological role of this irreversible uncoupling mechanism, if any, is unknown, but it conceivably might minimize the effects of lens injury by uncoupling damaged cells from healthy ones.

It is clear from the experiments reported here and those reported in the literature (4) that the lens-fiber junctions can be uncoupled under certain conditions. These conditions include chemical fixation and prolonged exposure to high pCO_2. Indeed, Spray et al. (36) have reported that there may be multiple gating mechanisms controlling gap-junction conductance. Unlike the uncoupling in embryonic junctions, this uncoupling of the lens-fiber junctions is generally not reversible and is accompanied by cell death. The resistance of lens fiber gap junctions to uncoupling by CO_2 may not be unique: Flagg-Newton and Loewenstein (11) have demonstrated a resistance to CO_2 blockage of intercellular dye transfer in cultured mammalian cells, not found in vertebrate or invertebrate organized tissues. Meyer and Revel (26) have reported that hepatocytes cannot be electrotonically uncoupled by increased pCO_2, although the critical experiments with dye transfer have not been reported. Thus, one can only conclude at this time that lens-fiber gap junctions show increased resistance to CO_2-induced uncoupling compared with embryonic lens gap junctions. It cannot yet be concluded that this CO_2-resistance is a unique property of the morphologically distinct class of gap junctions joining lens fibers.

The block of dye transfer between young lens cells is not accompanied by electrical uncoupling. One interpretation is that high pCO_2 effects a partial closure of all junctional channels so that the relatively large Lucifer yellow ions are excluded, but small inorganic ions are not, as suggested for intracellular calcium effects (24, 31). Alternatively, channels may be in an equilibrium between fully open and fully closed states, and elevated pCO_2 may shift the equilibrium towards channel closing (35). In this case, high pCO_2 is presumed to close enough junctional channels so that dye movement is too slow to be detected, but enough channels remain open to mediate measurable electrical coupling. In principle, one could discriminate between these models by measuring the rate of dye movement and junctional conductance as a function of pCO_2. If connexons have just two states, open and closed, then increasing pCO_2 should decrease dye transfer and junctional conductance in parallel. On the other hand, if CO_2 modulates channel aperture, raising the pCO_2 should block dye transfer completely before junctional conductance is lost. We could not do these experiments because we have no way to quantify the spread of Lucifer yellow within the lens or to measure junctional conductance.

Although we find a close temporal correlation between the observed morphological and physiological parameters of the junctions during development, there are two alternate explanations to our data which cannot be excluded and which are discussed below. As mentioned in Results, due to technical difficulties we have not attempted to quantify the absolute number of gap junctions per cell. Since freeze-fracture is not a random process, morphometric techniques cannot be properly applied to the replicas. It is possible that the number of gap junctions joining adjacent cells increases exponentially during the short (3-h) period of developmental time required for the observed change in dye transfer properties, and that a large

increase in channel number is responsible for the insensitivity to elevated CO_2. If channel closing is all-or-none at the single-channel level, one can argue that the CO_2-mediated uncoupling reflects an increase in the total number of connexons and not a change in connexon regulatory mechanisms. If high pCO_2 closes a constant fraction of connexons at all stages, the appearance of CO_2-resistant dye exchange might be a consequence of the larger absolute number of open connexons in the presence of CO_2. Although we cannot discard this alternative, we feel it to be less likely. The freeze-fracture replicas we have examined show no evidence of a nonlinear explosive assembly of large junctional surface areas during the critical 3 h of stage 14. Indeed, the transition is so abrupt that we cannot tell in any given stage-14 embryo whether the lens cells will be CO_2-sensitive or not without electrophysiological experimentation.

The second alternate interpretation of our results is that the loss of CO_2-sensitivity is due to an increased cellular buffering capacity. Thin-sections of stage-14 and -15 embryonic lenses show no apparent changes in cell organelles (e.g., mitochondria) which might influence intracellular buffering (data not shown). One could test this alternate interpretation by measuring intracellular pH as a function of pCO_2 in early and late developmental stages. We did not do this because embryonic lens cells are too small (~5–10 μm in diameter) to be impaled with both pH and reference microelectrodes simultaneously. Although we cannot exclude this explanation, we find it unlikely because one must also suppose that an increased buffering capacity directly parallels the appearance of dispersed connexons in freeze-fracture replicas.

Due to the very close temporal correlation between the changes in morphology and physiology of the junctions, the interpretation of our experiments which we favor is that lens fiber connexons are less sensitive than embryonic connexons to decreased intracellular pH. Unfortunately, there are no available biochemical data which permit a comparison of the polypeptide composition of the lens-fiber gap junctions with that of the embryonic gap junctions. Preliminary sequencing data (27) reveal a striking nonhomology between principal polypeptides isolated from lens-fiber and hepatocyte gap junctions; SDS PAGE of isolated myocardial gap junctions suggests the possibility of yet a third class (19). Taken together, it is possible that gap junctions between different cell types represent a spectrum of cellular interactions rather than a highly conserved structure. The meaning of this heterogeneity is not known, but it may reflect in part different regulatory or junction protein turnover requirements imposed by the unique physiological environments of the cells *in situ*.

We are grateful to Dr. W. Stewart for his generous gift of Lucifer yellow. We are indebted to Drs. E. Raviola and R. Dacheux for their advice, support, and friendship.

These studies were supported by grants EY02430 and EY03011 from the National Institutes of Health. S. M. Schuetze was supported by postdoctoral fellowship EY05337 and D. A. Goodenough by Career Development Award GM00231.

Received for publication 20 April 1981, and in revised form 8 September 1981.

REFERENCES

1. Adams, J. C. 1977. Technical considerations on the use of horseradish peroxidase as a neuronal marker. *Neuroscience*. 2:141–145.
2. Baldwin, K. M. 1979. Cardiac gap junction configuration after an uncoupling treatment as a function of time. *J. Cell. Biol.* 82:66–75.
3. Bennett, M. V. L., J. E. Brown, A. L. Harris, and D. C. Spray. 1978. Electrotonic junctions between *Fundulus* blastomeres: reversible block by low intracellular pH. *Biol. Bull. (Woods Hole)*. 155:428–429.
4. Bernardini, G., C. Peracchia, and R. A. Venosa. 1980. Uncoupling in lens fibers. *J. Cell Biol.* 87(2, Pt. 2): 207*a* (Abstr.).
5. Bloemendal, H. 1977. The vertebrate eye lens. *Science (Wash. D. C.)*. 197:127–138.
6. Cohen, A. I. 1965. The electron microscopy of the normal human lens. *Invest. Ophthalmol.* 4:433–446.
7. Dahl, G., and G. Isenberg. 1980. Decoupling of heart muscle cells: correlation with increased cytoplasmic calcium activity and with changes in nexal ultrastructure. *J. Membr. Biol.* 53:63–75.
8. Fallon, R. F., and D. A. Goodenough. 1981. Five-hour half-life of mouse liver gap junction protein. *J. Cell Biol.* 90:521–526.
9. Finbow, M., S. B. Yancey, R. Johnson, and J. P. Revel. 1980. Independent lines of evidence suggesting a major gap junctional protein with a molecular weight of 26,000. *Proc. Natl. Acad. Sci. U. S. A.* 77:970–974.
10. Flagg-Newton, J., I. Simpson, and W. R. Loewenstein. 1979. Permeability of the cell-to-cell membrane channels in mammalian cell junction. *Science (Wash. D. C.)*. 205:404–407.
11. Flagg-Newton, J., and W. R. Loewenstein. 1979. Experimental depression of junctional membrane permeability in mammalian cell culture. A study with tracer molecules in the 300 to 800 dalton range. *J. Membr. Biol.* 50:65–100.
12. Goodenough, D. A. 1979. Lens gap junctions: a structural hypothesis for non-regulated low resistance intercellular pathways. *Invest. Ophthalmol.* 18:1104–1122.
13. Graham, R. C., and M. J. Karnovsky. 1966. The early stages of absorption of injected horseradish peroxidase in the proximal tubules of mouse kidney: ultrastructural cytochemistry by a new technique. *J. Histochem. Cytochem.* 14:291–302.
14. Hamburger, V., and H. L. Hamilton. 1951. A series of normal stages in the development of the chick embryo. *J. Morphol.* 88:49–92.
15. Hamilton, H. L. 1965. Lillie's Development of the Chick. An Introduction to Embryology. 3rd Edition. Holt, Rinehart and Winston, New York.
16. Henderson, D., H. Eibl, and K. Weber. 1979. Structure and biochemistry of mouse hepatic gap junctions. *J. Mol. Biol.* 132:193–218.
17. Hertzberg, E. L., and N.B. Gilula. 1979. Isolation and characterization of gap junctions from rat liver. *J. Biol. Chem.* 254:2138–2147.
18. Kensler, R. W., P. Brink, and M. M. Dewey. 1977. Nexus of frog ventricle. *J. Cell Biol.* 73: 768–781.
19. Kensler, R. W., and D. A. Goodenough. 1980. Isolation of mouse myocardial gap junctions. *J. Cell Biol.* 86:755–764
20. Kistler, J., and S. Bullivant. 1980. The connexon order in isolated lens gap junctions. *J. Ultrastruct. Res.* 72:27–38.
21. Kuszak, J., H. Maisel, and C. V. Harding. 1978. Gap junctions of chick lens fiber cells *Exp. Eye Res.* 27:495–498.
22. Kuwabara, T. 1975. The maturation of the lens cell: a morphological study. *Exp. Eye Res.* 20:427–443.
23. Lo, C. W., and N. B. Gilula. 1979. Gap junctional communication in the preimplantation mouse embryo. *Cell.* 18: 399–409.
24. Loewenstein, W. R., Y. Kanno, and S. J. Socolar. 1978. Quantum jumps of conductance during formation of membrane channels at cell-cell junction. *Nature (Lond.)*. 274:133–136.
25. Malmgren, L. T., and Y. Olsson. 1977. A sensitive histochemical method for light- and electron-microscopic demonstration of horseradish peroxidase. *J. Histochem. Cytochem.* 25:1280–1283.
26. Meyer, D. J., and J. P. Revel. 1981. CO_2 does not uncouple hepatocytes in the rat liver. *Biophys. J.* 33(2, Pt. 2):195a (Abstr.).
27. Nicholson, B. J., M. W. Hunkapiller, L. E. Hood, and J. P. Revel. 1980. Partial sequencing of the gap junctional protein from rat lens and liver. *J. Cell Biol.* 87(2, Pt. 2):200*a* (Abstr.).
28. Peracchia, C., and L. L. Peracchia. 1980. Gap junction dynamics: reversible effects of divalent cations. *J. Cell Biol.* 87:708–718.
29. Peracchia, C., and L. L. Peracchia. 1980. Gap junction dynamics: reversible effects of hydrogen ions. *J. Cell Biol.* 87:719–727.
30. Raviola, E., D. A. Goodenough, and G. Raviola. 1980. Structure of rapidly frozen gap junctions. *J. Cell Biol.* 87:273–279.
31. Rose, B., I. Simpson, and W. R. Loewenstein. 1977. Calcium ion produces graded changes in permeability of membrane channels in cell junction. *Nature (Lond.)*. 267:625–627.
32. Turin, L., and A. Warner. 1977. Carbon dioxide reversibly abolishes ionic communication between cells of early amphibian embryo. *Nature (Lond.)*. 270:56–57.
33. Turin, L., and A. E. Warner. 1980. Intracellular pH in early *Xenopus* embryos: its effects on current flow between blastomeres. *J. Physiol. (Lond.)*. 300:489–504.
34. Simpson, I., B. Rose, and W. R. Loewenstein. 1977. Size limit of molecules permeating the junctional membrane channels. *Science (Wash. D. C.)*. 195:294–297.
35. Spray, D. C., A. L. Harris, and M. V. L. Bennett. 1981. Gap junctional conductance is a simple and sensitive function of intracellular pH. *Science (Wash. D. C.)*. 211:712–715.
36. Spray, D. C., A. L. Harris, and M. V. L. Bennett. 1981. Glutaraldehyde differentially affects gap junction conductance and its pH and voltage dependence. *Biophys. J.* 33(2, Pt. 2):108a (Abstr.).
37. Yancey, S. B., B. J. Nicholson, and J. P. Revel. 1981. The gap junction protein, partial sequence and turnover. *J. Supramol. Struct. Suppl.* 5:312.